Supplementary Information

Unpoppable Bubble

Weikang Lin[1,2†], Yi Zheng[1,2†], Jigang Feng[3†], Yunfei Liu[3], Xiaodan Yang[1,2], Zhaoye Qin[3], Zhengbao Yang[1*]

Corresponding to: zbyang@ust.hk

Table of contents:

1.Double spring-mass model for the vibration bubble system

Initially, the system consists of a sessile droplet partially wetting a planar solid support, which is vertically vibrated at a frequency of $\omega/2\pi$ with an amplitude A_c (**Supplementary Fig. 1a**). The vibration damping characteristics of the sessile droplet system are illustrated in **Supplementary Fig. 1b**, showing that m_1 and m_2 were connected with an infinite K_2. For the sessile droplet system, the differential equation of motion can be expressed as: $m\ddot{x} + C_1\dot{x} + K_1x = F_0\sin\ \omega t$. The displacement of the droplet satisfies $x = X\sin(\omega t - \varphi)$, where X, ω, φ represent the amplitude, angular frequency, and phase of the forcing, respectively. Thus, the amplitude of the forcing vibration can be calculated as:

$$X = \frac{F_0}{\sqrt{(K_1 - m\omega^2)^2 + (C_1\omega)^2}} \tag{1}$$

The sessile bubble system can be divided into two parts: the platform with m_1, K_1, C_1, as the primary system and the bubble with m_2, K_2, C_2 as the damper (**Supplementary Fig. 1c**). The differential equations of motion for this system are:

$$m_1\ddot{x}_1 + (C_1 + C_2)\dot{x}_1 - C_2\dot{x}_2 + (K_1 + K_2)x_1 - K_2x_2 = F_1\sin\omega t \tag{2}$$

$$m_2\ddot{x}_2 - C_2\dot{x}_1 + C_2\dot{x}_2 - K_2x_1 + K_2x_2 = 0 \tag{3}$$

The displacement of the platform and the bubble can be expressed as:

$$x_1(t) = X_1\mathrm{e}^{\mathrm{i}(\omega t - \varphi)} \tag{4}$$

$$x_2(t) = X_2\mathrm{e}^{\mathrm{i}(\boldsymbol{\omega} t - \boldsymbol{\varphi})} \tag{5}$$

Given that the damping C_1 is relatively low and can be neglected, the formulation can be simplified as:

$$\begin{bmatrix} K_1 + K_2 - \omega^2 m_1 + \mathrm{i}\omega C_2 & -(K_2 + \mathrm{i}\omega C_2) \\ -(K_2 + \mathrm{i}\omega C_2) & K_2 - \omega^2 m_2 + \mathrm{i}\omega C_2 \end{bmatrix} \begin{bmatrix} X_1\mathrm{e}^{-\mathrm{i}\varphi} \\ X_2\mathrm{e}^{-\mathrm{i}\varphi} \end{bmatrix} = \begin{bmatrix} F_1 \\ 0 \end{bmatrix} \tag{6}$$

The determinant of the matrix $\mathbf{Z}(\omega)$ is:

$$\begin{aligned} \det[\mathbf{Z}(\omega)] &= \begin{vmatrix} K_1 + K_2 - \omega^2 m_1 + \mathrm{i}\omega C_2 & -(K_2 + \mathrm{i}\omega C_2) \\ -(K_2 + \mathrm{i}\omega C_2) & K_2 - \omega^2 m_2 + \mathrm{i}\omega C_2 \end{vmatrix} \\ &= (K_1 - \omega^2 m_1)(K_2 - \omega^2 m_2) - \omega^2 K_2 m_2 \\ &\quad + \mathrm{i}\omega C_2(K_1 - \omega^2 m_1 - \omega^2 m_2) \end{aligned} \tag{7}$$

The solutions for X_1 and X_2 are as follows:

$$X_1 = F_1\sqrt{\frac{(K_2 - \omega^2 m_2)^2 + \omega^2 {C_2}^2}{[(K_1 - \omega^2 m_1)(K_2 - \omega^2 m_2) - \omega^2 K_2 m_2]^2 + \omega^2 {C_2}^2 (K_1 - \omega^2 m_1 - \omega^2 m_2)^2}} \tag{8}$$

$$X_2 = F_1\sqrt{\frac{K_2^2 + \omega^2 {C_2}^2}{[(K_1 - \omega^2 m_1)(K_2 - \omega^2 m_2) - \omega^2 K_2 m_2]^2 + \omega^2 {C_2}^2 (K_1 - \omega^2 m_1 - \omega^2 m_2)^2}} \tag{9}$$

Upon transformation into dimensionless form, the displacement of platform x_1 can be written as:

$$x_1 = \frac{F_1}{K_1}\sqrt{\frac{(a^2-\lambda^2)+(2\xi\lambda)^2}{(1-\lambda^2)(a^2-\lambda^2)-\mu(a\lambda)^2+(2\xi\lambda)^2(1-\lambda^2-\mu\lambda^2)^2}} \tag{10}$$

Where, $\mu = \frac{m_2}{m_1}$, $\alpha = \frac{\omega_2}{\omega_1}$ $\lambda = \frac{\omega}{\omega_1}$, m_1 and m_2 represent the mass of the bubble and platform, respectively. In this experiment, $\mu = 1/40$, and $\xi = 0.025$. ω_1 and ω_2 are the natural frequency of the system measured through the free decay test (**Supplementary Fig. 1d** and **e**).

The theoretical curve for the platform's displacement x_1 can be obtained from the above expressions, as shown in **Supplementary Fig. 1f**, matching the trend observed in the experimental data.

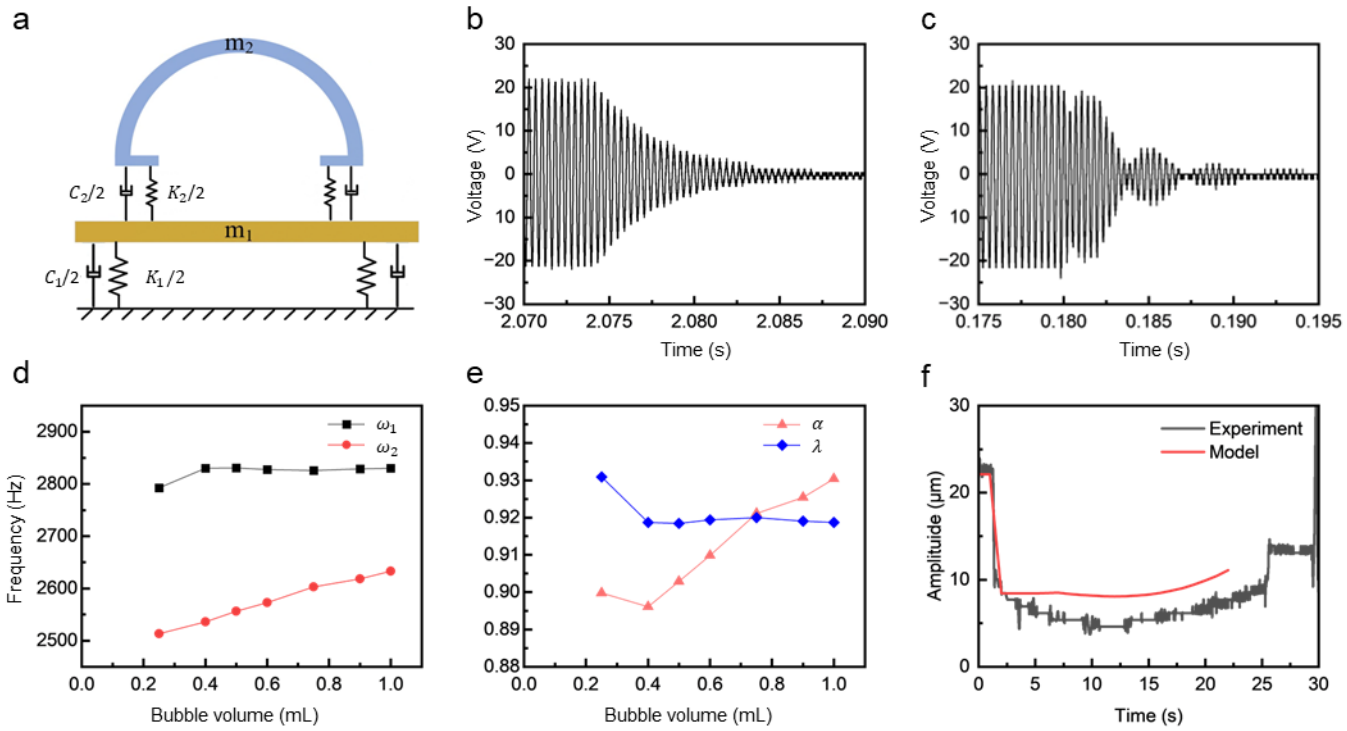

Supplementary Fig. 1: Dynamic analysis of the bubble vibration system. a, Schematic of the double-spring system that depicts the bubble vibration system. **b** and **c**, The vibration damping characteristics of the sessile droplet system (**b**) and the bubble system (**c**). **d**, The natural frequency ω_1 and ω_2.of the system in different bubble size. **e**, The parameter $\alpha = \omega_2/\omega_1$ and $\lambda = \omega/\omega_1$ in different bubble size. **f**, Vertical amplitude of the bubble system. The experimental data (black line) are fitted by the double spring-mass model with fitting parameters (red line).

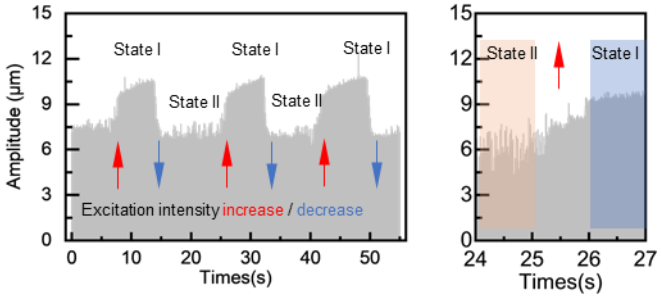

Supplementary Fig. 2: Bubble state transition verse excitation intensity. The amplitude of the vibration system changed with the excitation intensity leading to the state reverse transition. Increasing the excitation intensity promotes the bubble state change from oscillation state **II** to static state **I**.

2. Stabilization of the air bubble by vertical oscillation

In the classical Kapitza's pendulum model (**Supplementary Fig. 2a**), when the pendulum is subjected only to gravity, the equation of motion is given by $ml\ddot{\theta} + mg\theta = 0$. It is evident that the system is unstable when $\theta = \pi$, the system is unstable.

Upon applying vertical vibration to the pendulum, $y = A_0\, cos(\omega t)$, the dynamic equation becomes:

$$ml\ddot{\theta} + mg\theta = m\ddot{y}\, sin\, \theta \tag{11}$$

The acceleration due to vibration is $\ddot{y} = -A_0\omega^2\, cos(\omega t)$, leading to the dynamic equation:

$$ml\ddot{\theta} + mg\theta = -mA_0\omega^2\, cos(\omega t)\, sin\, \theta \tag{12}$$

After the small-angle approximation $sin\, \theta \approx \theta$ and averaging Mathieu's equation[1–4], we obtain

$$\ddot{\theta} + \left(g - \frac{{A_0}^2\omega^2}{2l}\right)\theta = 0 \tag{13}$$

The system remains stable as long as the following condition is satisfied:

$${A_0}^2\omega^2 > 2lg \tag{14}$$

For the bubble model (**Supplementary Fig. 2a**), the liquid film at the bubble cap can be viewed as a high-density liquid layer floating on low-density air, akin to Rayleigh-Taylor instability. Madison S. Krieger studied a scenario involving two unbounded, incompressible, immiscible fluids that share a common interface. In this model, the position of the interface is denoted by $\zeta(x, y, t)$, with the neglect of liquid viscosity and surface tension. Given that the speeds at the interface are small when stable, Bernoulli's principle can be linearized regarding the unsteady heads at the interface, leading to the equation $\ddot{\zeta} = Agk\zeta$, which resembles a simple harmonic oscillator. When a vertical vibration $y = A_0\, cos(\omega t)$ is applied to the system, the stability criterion for the trivial solution becomes[5,6]:

$$k{A_0}^2\omega^2 > 2gA \tag{15}$$

Furthermore, Benjamin Apffel[3] derived the perturbation equation considering surface tension:

$$\ddot{\zeta} + \left(\lambda^2 + \frac{k^2 {A_0}^2 \omega^2}{2}\right)\zeta = 0 \tag{16}$$

Where $\lambda^2 = -\left(Agk - \frac{\gamma k^3}{\rho_A + \rho_L}\right)$, k is wave number, γ is surface tension, $A = \frac{\rho_L - \rho_A}{\rho_L + \rho_A}$, and ρ_A, ρ_L are the density of air and liquid.

The stability condition for the trivial solution ζ=0 is:

$$\frac{k^2 {A_0}^2 \omega^2}{2} > \lambda^2 \tag{17}$$

In our bubble mode, the effect of gravity and capillary drive the bubble system toward instability. Here, λ^2 is defined as $-\left(Agk + \frac{\gamma k^3}{\rho_A + \rho_L}\right)$, and the traivial solution is given by the inequality:

$$A_0\omega > \sqrt{2\frac{Ag}{k} + \frac{2\gamma \mathrm{k}}{\rho_A + \rho_L}} \tag{18}$$

Hence, in the bubble system, the wavenumber $k \sim 1/r$, where r is the radius of the bubble. Taking into account that the air density ρ_A is significantly smaller compared to the liquid density ρ_L, ρ_A can be neglected. Moreover, for big bubbles, the capillary effect dominates gravity to the extent that gravity can also be neglected[7], we can derive the critical velocity for the stability of bubbles:

$$v = A_0\omega > \sqrt{k} \times \sqrt{\frac{2\gamma}{\rho_L}} \tag{19}$$

It's important to note that our experimental vibration platform involves forced vibration of a uniform circular clamped plate at frequencies near resonance frequency, satisfying $A_0/A_\mathrm{c} = (1 - (r/\mathrm{R})^2)^2$, where R is the active radius, A_0 is the amplitude at radius r, and A_c is the amplitude at the central point. In addition, assuming the bubble shape is a semisphere, the bubble radius is $r = \sqrt[3]{3V/2\pi}$ where V is the bubble volume. The critical stability velocity is then given by:

$$v = A_\mathrm{c}\omega > \sqrt{k} \times \sqrt{\frac{2\gamma}{\rho_L}} \times \frac{1}{\left(1 - \left(\frac{r}{\mathrm{R}}\right)^2\right)^2} \tag{20}$$

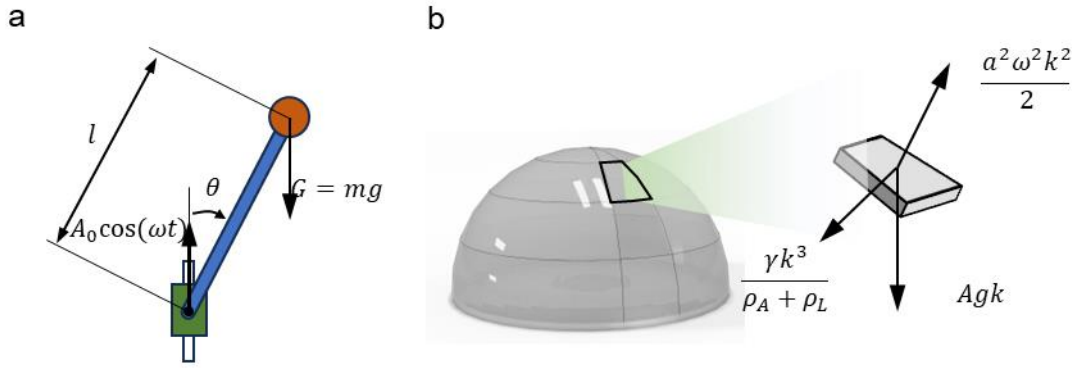

Supplementary Fig. 3: Mechanism of the bubble statbility. a, Schematic of the Kapitza pendulum. **b**, Schematic of the force balance at the air-liquid interface. The force induced by the vibration effect cancels the gravity and capillary force.

3. Simulation

To further validate the hypothesis of vibration-induced stability, a computational fluid dynamics (CFD) analysis of a liquid thin film was conducted using COMSOL Multiphysics 6.1. The model was specifically designed to represent the hydrodynamic conditions within a partial liquid membrane of a bubble subjected to oscillatory forces. Two-dimensional models are employed to minimize the computational complexity.

A rectangular fluid domain, measuring 1 mm in length and 0.1 mm in thickness, was established to simulate the thin film. The built-in properties of *Water (liquid)* were directly employed as the liquid material. The *Laminar Flow (spf)* module was utilized to compute the dynamics of the liquid thin film, governed by the Navier-Stokes equations and the continuity equation. The longer edges of the domain, representing the internal and external surface of the bubble, were defined as interfacial surfaces between water and air. For the shorter left and right edges, *Prescribed Normal Displacements* were applied to replicate the transmitted vibration sources. These edges oscillated sinusoidally at a frequency of 2600 Hz and an amplitude of 30 μm, as measured experimentally. For consistency, the short edges were set to move synchronously and in-phase, and gravitational effects were included in the model.

A structured quadrilateral mesh was generated within the computational domain to ensure adequate spatial resolution, resulting in a total of 12,150 elements were in the final configuration. Additionally, the *Moving Mesh* module was incorporated into the model to accurately represent the surface deformation of the bubble. Simulations were performed using the time-dependent solver, predicting the velocity filed and surface fluctuations over the initial 40 periods of oscillation.

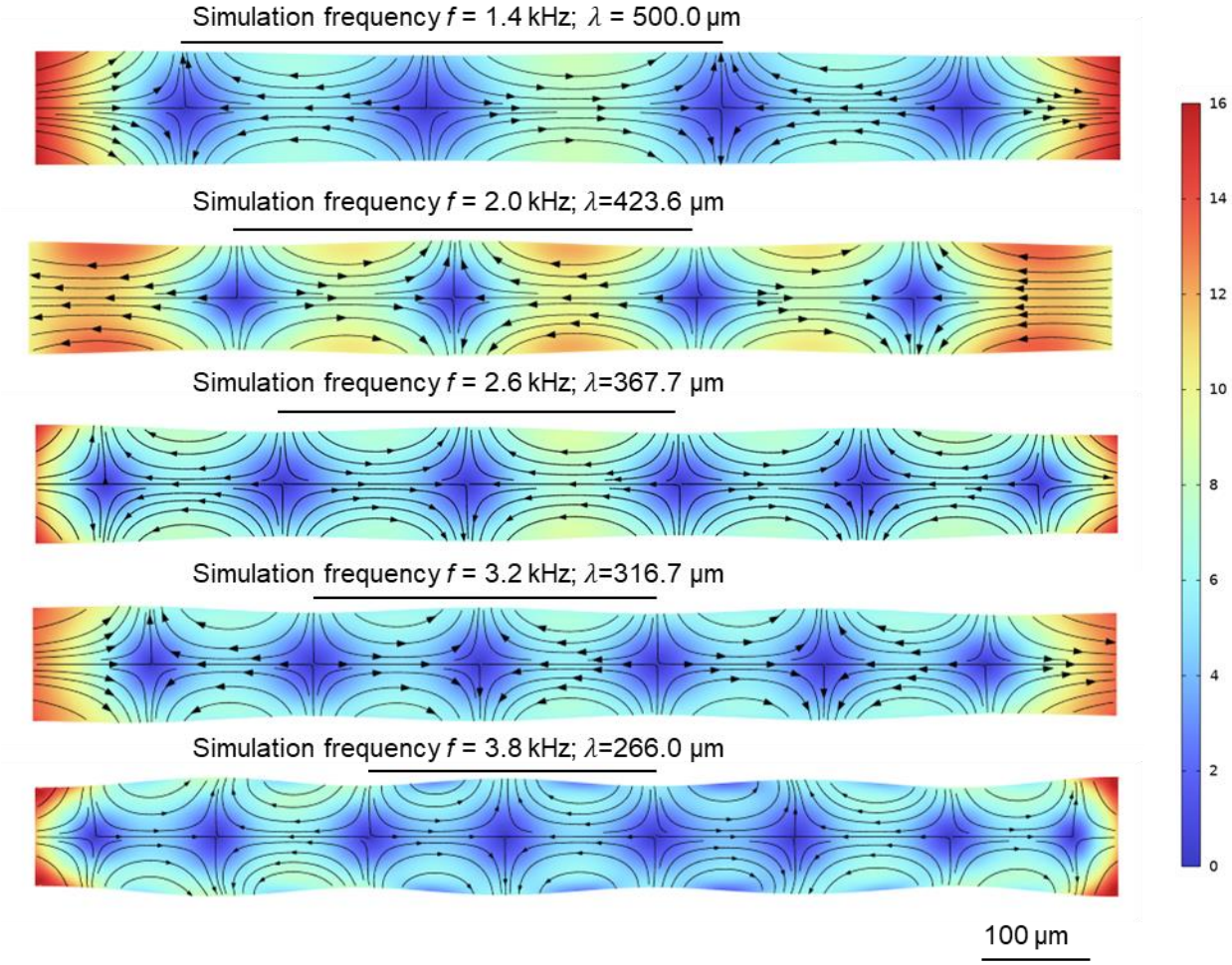

Supplementary Fig. 4: The wavelength of the wrinkle under different vibration frequencies.

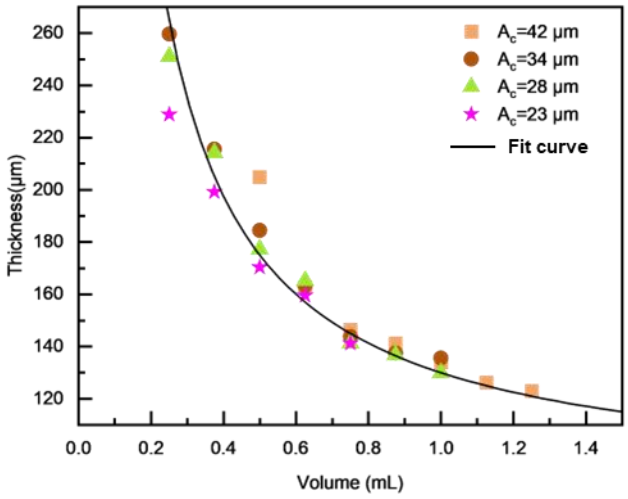

Supplementary Fig. 5: Effect of vibration intensity and bubble size on bubble thickness.

1. Martín, E., Martel, C. & Vega, J. M. Drift instability of standing Faraday waves. *J. Fluid Mech.* **467**, 57–79 (2002).
2. Rayleigh, J. W. S. *The Theory of Sound*. vol. 2 (Dover Publications, 1945).
3. Apffel, B., Novkoski, F., Eddi, A. & Fort, E. Floating under a levitating liquid. *Nature* **585**, 48–52 (2020).
4. Troyon, F. & Gruber, R. Theory of the dynamic stabilization of the Rayleigh-Taylor instability. *Phys. Fluids* **14**, 2069–2073 (1971).
5. Bajaj, R. & Malik, S. K. Parametric instability of the interface between two viscous magnetic fluids. *J. Magn. Magn. Mater.* **253**, 35–44 (2002).
6. Horsley, D. E. & Forbes, L. K. A spectral method for Faraday waves in rectangular tanks. *J. Eng. Math.* **79**, 13–33 (2013).
7. Oratis, A. T., Bush, J. W. M., Stone, H. A. & Bird, J. C. A new wrinkle on liquid sheets: Turning the mechanism of viscous bubble collapse upside down. *Science (80-.).* **369**, 685–688 (2020).